Chinese Chemical Letters 36 (2025) 109923

Contents lists available at ScienceDirect

Chinese Chemical Letters

journal homepage: www.elsevier.com/locate/cclet

Biisoindolylidene solvatochromic fluorophores: Synthesis and photophysical properties

Xiaoyu Chen[a,b,c], Jiahao Hu[a,b,c], Jingyi Lin[a,b,c], Haiyang Huang[b], Changqing Ye[b,**], Hongli Bao[b,c,d,*]

[a] College of Chemistry, Fuzhou University, Fuzhou 350108, China
[b] State Key Laboratory of Structural Chemistry, Key Laboratory of Coal to Ethylene Glycol and Its Related Technology, Center for Excellence in Molecular Synthesis, Fujian Science & Technology Innovation Laboratory for Optoelectronic Information of China, Fuzhou 350116, China
[c] Fujian College, University of Chinese Academy of Sciences, Fuzhou 350002, China
[d] University of Chinese Academy of Sciences, Beijing 100049, China

ARTICLE INFO

Article history:
Received 7 February 2024
Revised 5 April 2024
Accepted 24 April 2024
Available online 25 April 2024

Keywords:
Biisoindolylidene
Electron receptor
New fluorophores
Solvatochromic
Acid sensitive

ABSTRACT

Environment-sensitive fluorescent probes are commonly utilized in various fields, including fluorescence sensing and imaging. This paper describes the synthesis and photophysical properties of a novel class of solvatochromic fluorophores that incorporate biisoindolylidene as the core backbone. This study investigates the structure-property relationships of these newly developed fluorophores. The central biisoindolylidene acts as an efficient electron acceptor, and by modifying the aryl ring substituent at the 3,3′ position, the photophysical properties of the fluorophores can be significantly enhanced, particularly in terms of photoluminescence quantum efficiency. Furthermore, when an electron-donor group replaces the aryl ring at the 3,3′ position, intriguing solvatochromic behavior is observed. This leads to a red-shift in the maximum emission wavelength and an increase in the Stokes shift with increasing solvent polarity. In solvent dimethyl sulfoxide (DMSO), the maximum emission wavelength can reach up to 750 nm, with a Stokes shift of approximately 150 nm. Finally, the potential application of the fluorophore in the detection of volatile acids is explored in a preliminary manner.

Environment-sensitive fluorescent probes are a specific category of dyes that are designed to track changes in the environment by detecting alterations in fluorescence intensity or color [1–3]. A variety of fluorophores have been developed for monitoring pH [4–7], reactive oxygen species (ROS) [8,9], viscosity [10], ions [6,11,12], bioconjugation reaction [13,14], cellular organelles [15,16], polarity [17] *etc.* These fluorophores operate through mechanisms such as charge transfer, twisted intramolecular charge transfer [18,19], intramolecular proton transfer [20], conformational changes [21,22], and changes in aggregation states [23]. AIEgen, for example, which has a rotatable molecular structure, serves as an efficient probe for tracking microenvironmental viscosity and aggregation states [24–26]. Moreover, fluorophores with dynamic molecular structures can measure changes in free volume in polymer matrices. There are also other fluorophores available for monitoring extremely harsh environments, such as high pressure or high temperature [27,28]. Solvatochromic dyes, which fall under this category, are capable of changing their color in response to the polarity of the solvent [29,30].

Classical solvatochromic dyes that consist of both donor and acceptor moieties, known as push-pull fluorophores [31]. This push-pull structure facilitates the transfer of charge from the donor moiety to the acceptor upon light absorption, leading to the formation of a highly dipolar excited state. The excited state, which is highly dipolar, interacts with the dipole of the solvent and relaxes, resulting in a redshift in wavelength in solvents with high polarity. Various push-pull dyes, such as Prodan [32,33], Dansyl [34], Anthradan [35], FR0 [36], PA [37,38], 4DMP [39], NBD [40], Coumarine 153, Dapoxyl [41], Nile Red, DCDHF-6 [42] and 3MC-2 (Fig. 1a) [43], have been extensively studied in the literature. However, the selection of the most suitable fluorescent tool requires careful consideration of several factors, including quantum yield, absorption and emission wavelengths, photostability, chemical stability, and Stokes shift. To address these requirements, scientists have designed a variety of dyes with distinct structural features. Each dye presents

* Corresponding author at: State Key Laboratory of Structural Chemistry, Key Laboratory of Coal to Ethylene Glycol and Its Related Technology, Center for Excellence in Molecular Synthesis, Fujian Science & Technology Innovation Laboratory for Optoelectronic Information of China, Fuzhou 350116, China.
** Corresponding author.
E-mail addresses: qzycq@fjirsm.ac.cn (C. Ye), hlbao@fjirsm.ac.cn (H. Bao).

https://doi.org/10.1016/j.cclet.2024.109923
1001-8417/

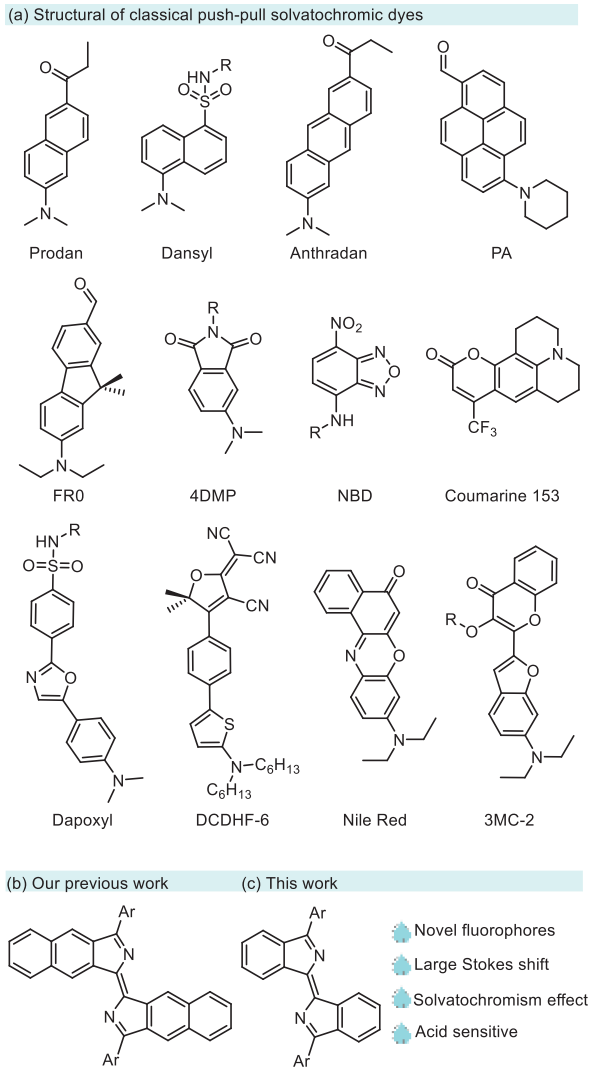

Fig. 1. (a) Structural of classical push−pull solvatochromic dyes. (b) Our previous work. (c) This work.

its own set of advantages and disadvantages, which must be carefully evaluated for specific applications. Consequently, the continuous development of new small molecule probes is crucial to encompass all necessary elements while minimizing compromises [44].

The development of new solvatochromic dyes currently relies on modifying existing fluorophores. In a recent study, we reported a series of bisbenzo[*f*]isoindolylidenes compounds from dipropargyl benzenesulfonamides (Fig. 1b) [45]. Through the modification of dipropargyl benzenesulfonamides, herein we have successfully synthesized a series of novel biisoindolylidene compounds (Fig. 1c). In comparison to previous work, the new probes also offer the advantage of tunable emission and superior photostability. Furthermore, these new probes exhibit large stokes shift and more sensitive environmental responses. By introducing an electron-donating group at the 3,3′ position, it becomes feasible to transition the excited state of these compounds from a locally excited state to a charge-transfer excited state, resulting in remarkable solvatochromic properties.

With **1s** as the model substrate, we optimized the conditions for the synthesis of (*E*)-3,3′-diphenyl-1,1′-biisoindolylidene (**1**). Various catalysts were screened using K_2CO_3 as a base and ^{n}BuOH as a solvent at 80 °C in the presence of air (Table 1, entries 1–4). The dimeric product **1** could be obtained in 33% yield without any catalyst (Table 1, entry 5). None of the other bases and solvents resulted in an improvement in the reaction yield (Table 1, entries 6–13). Interestingly, the use of NaClO as a co-oxidant increased the yield of the target product **1** to 41% (Table 1, entry 14). Furthermore, altering the temperature did not have any significant impact on the yield of product **1** (Table 1, entries 15–17).

Table 1
Reaction condition optimization.[a]

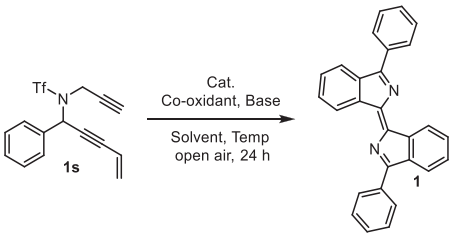

Entry	Cat.	Temp (°C)	Oxidant	Base	Solvent	Yield (%)
1	FePC	80	/	K_2CO_3	^{n}BuOH	10
2	Fe(heme)Cl	80	/	K_2CO_3	^{n}BuOH	13
3	CuBr	80	/	K_2CO_3	^{n}BuOH	25
4	CuTc	80	/	K_2CO_3	^{n}BuOH	26
5	–	80	/	K_2CO_3	^{n}BuOH	33
6	–	80	/	Cs_2CO_3	^{n}BuOH	trace
7	–	80	/	Et_3N	^{n}BuOH	20
8	–	80	/	KO^{t}Bu	^{n}BuOH	trace
9	–	80	/	DMAP	^{n}BuOH	7
10	–	80	/	DBU	^{n}BuOH	trace
11	–	80	/	K_2CO_3	DMSO	10
12	–	80	/	K_2CO_3	DMF	/
13	–	80	/	K_2CO_3	IPA	29
14	–	80	NaClO	K_2CO_3	^{n}BuOH	41
15	–	40	NaClO	K_2CO_3	^{n}BuOH	26
16	–	60	NaClO	K_2CO_3	^{n}BuOH	33
17	–	100	NaClO	K_2CO_3	^{n}BuOH	26

[a] Reaction conditions: **1s** (0.2 mmol, 1 equiv.), base (0.4 mmol, 2 equiv.), co-oxidant (0.4 mmol, 2 equiv.), solvent (1 mL).

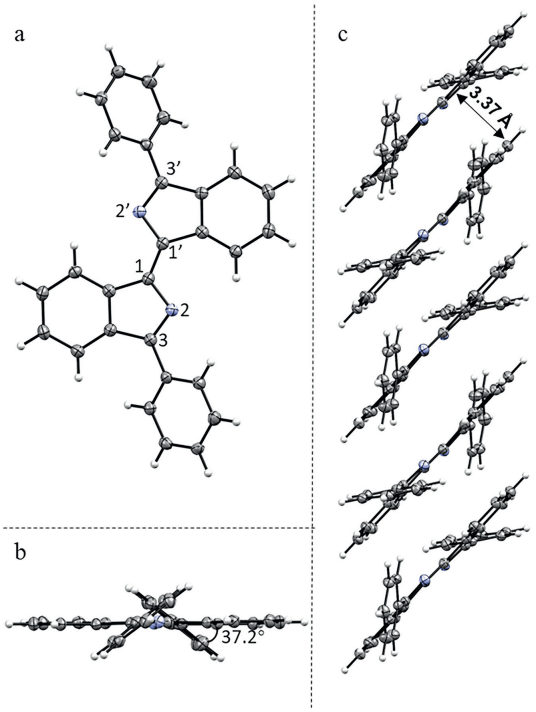

Fig. 2. (a, b) Crystal structure of compound **1**. (c) Packing model in the solid state of compound **1**.

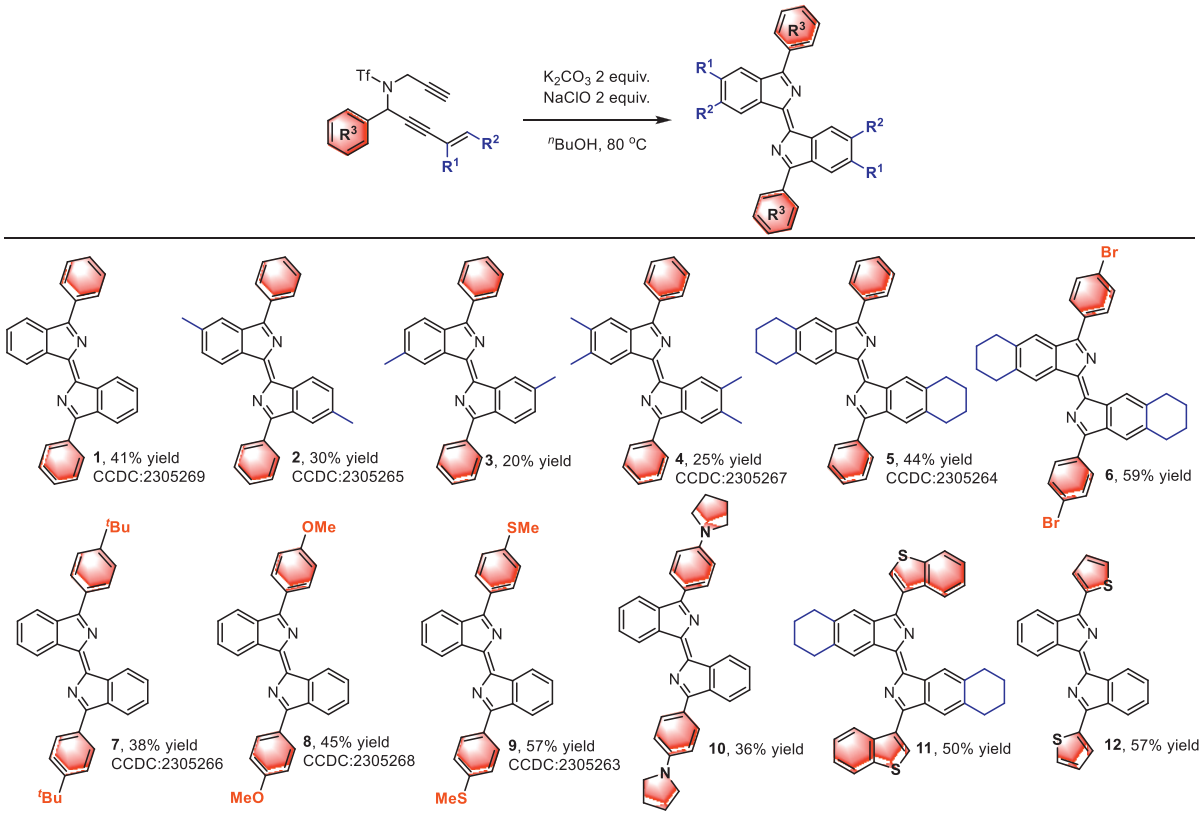

Fig. 3. Substrate scope. Reaction conditions: Dipropargyl trifluoromethanesulfonamide (0.2 mmol), K_2CO_3 (0.4 mmol), NaClO (aqueous solution containing 8% effective chlorine), ^{n}BuOH (1 mL), 80 °C, 24 h.

The structures of compound **1** was confirmed using X-ray crystallography. The crystal structure shown in Fig. 2, compound **1** is observed to be a rigid and coplanar compound with C_{2h} symmetry in its solid state. The dihedral angle between the phenyl group and the biisoindolylidene skeleton is measured to be 37.2°. The packing model reveals that both molecules are closely packed together in a *J*-type aggregation, with a distance of approximately 3.37 Å between neighboring molecules, indicating π-π surface overlap (Fig. 2c). The phenyl group at the 3,3′-position effectively extends the π-conjugation of the biisoindolylidene skeleton, providing electronic diversity. Consequently, modifying substituent groups, specifically the aryl substituent groups at the 3,3′-position, allows for the synthesis of various intriguing biisoindolylidene derivatives with distinct photophysical properties [46].

Based on the results of condition screening and crystal analysis, we synthesized a series of biisoindolylidene derivatives with various substituents in moderate yields (Fig. 3). Subsequently, we investigated their UV–vis absorption spectra, fluorescence spectra, and photoluminescence quantum yield in DCM. As shown in Fig. 3 and Table 2, the photophysical properties of the compounds **1**–**5** remained largely unchanged when substituent groups R^1 and R^2 were altered. The compounds exhibited a maximum absorption wavelength around 450 nm, while the maximum emission wavelengths ranged from 545 nm to 584 nm. However, the photoluminescence quantum yield was found to be very low. The introduction of bromine atoms (**6**) on the benzene ring of R^3 did not significantly affect the photophysical properties. In contrast, the introduction of an electron-donating group on R^3 resulted in noticeable changes in photophysical properties (**7**–**10**). The emission wavelength of the compounds gradually red-shifted, the photoluminescence quantum (PLQY) efficiency was significantly improved, and have a large Stokes shift (reached a maximum of 138 nm). Furthermore, the introduction of an electron-rich thiophene group in R^3 also led to significant changes in photophysical properties (**11** and **12**). These findings suggest that the substitution at 3,3′-position does have a significant effect on the photophysical properties of biisoindolylidene derivatives. Additionally, the structure of compounds **2**, **4**, **5**, **7**, **8**, and **9** were also confirmed by X-ray single crystal diffraction.

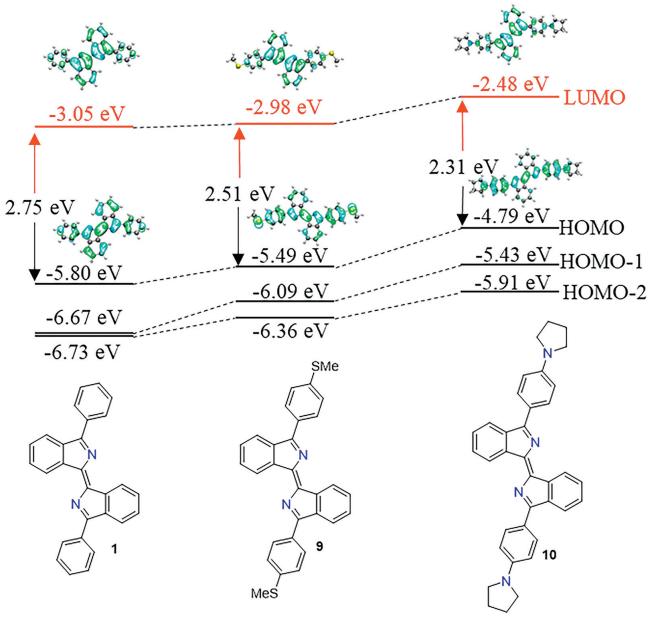

Fig. 4. Energy diagrams and pictorial representations of compounds **1**, **9** and **10** calculated at the B3LYP/6–31G(d,p) level.

Table 2
Optical data for compounds **1**–**12**.

Compound	$\lambda_{abs,max}$ (nm)	$\lambda_{em,max}$ (nm)	$\Delta\nu$ (cm^{-1})	Φ (%)
1	450	545	3874	1.2
2	450	558	4301	0.5
3	450	572	4740	0.4
4	450	584	5099	0.1
5	460	574	4318	0.1
6	450	584	5099	0.1
7	460	564	4009	10.1
8	480	588	3827	11.4
9	493	603	3700	30.3
10	565	698	3372	30.4
11	485	575	3227	9.8
12	500	598	3278	45.6

[a] Maximum absorption wavelength in DCM (10^{-5} mol/L).
[b] Maximum emission wavelength (excited by the maximum absorption wavelength) in DCM (10^{-5} mol/L).
[c] Photoluminescence quantum yield in DCM (10^{-5} mol/L).

To investigate the impact of substituents on orbital energies, we conducted DFT theoretical calculations using the B3LYP/6–31G(d,p) [47] level for compounds **1**, **9**, and **10** (Fig. 4). The HOMO energy levels of compounds **9** and **10**, which had electron-donating groups at the terminal aromatics, increased by 0.31 eV and 0.83 eV, respectively, compared to compound **1**. Consequently, the energy gap of compounds **9** and **10** were reduced to 2.51 eV and 2.31 eV, respectively. These findings suggest that the HOMO of this π-conjugated skeleton is significantly influenced by the terminal aryl groups. Compound **1** exhibits local excitation (LE) character as both its HOMO and LUMO are completely delocalized over the conjugation plane. On the other hand, the LUMOs of compounds **9** and **10** are distributed on the biisoindolylidene backbone, indicating its high electron-accepting properties. In contrast, the HOMO is mainly distributed on the electron-donor substituted aryl group at the 3,3′-position and the conjugated structure. The observed charge separation from the distribution of HOMO and LUMO suggests that the HOMO/LUMO transitions of compounds **9** and **10** exhibit charge transfer (CT) character.

The solvatochromic properties of compounds **1**, **9**, and **10** were investigated in different polar solvents, based on their calculated LE or CT character (Fig. 5 and Table 3) [48]. Compound **1** exhibited no significant change in emission wavelength (Figs. 5d and g), whereas compounds **9** and **10** displayed a red-shift in their

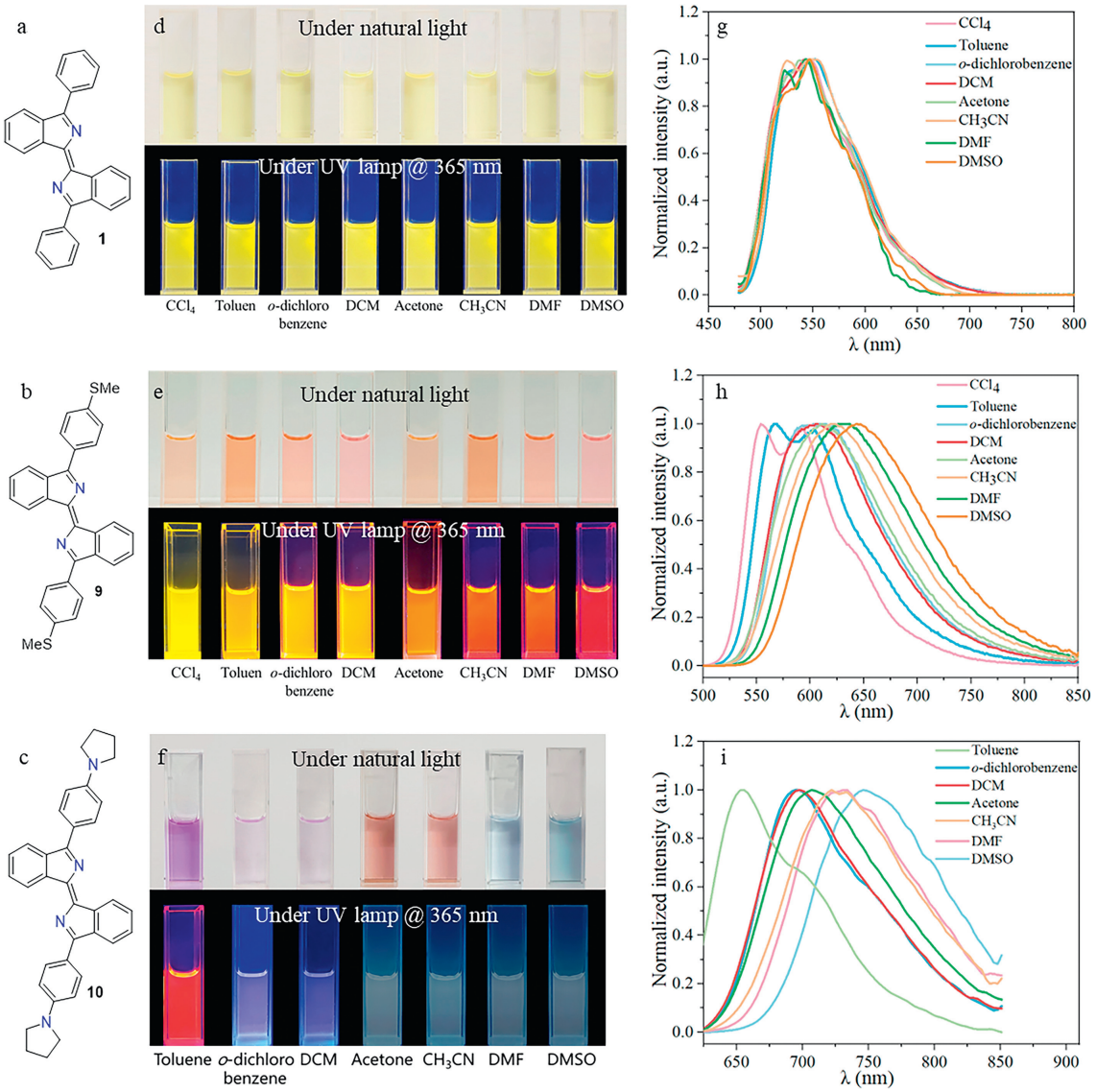

Fig. 5. (a–c) Structures of compounds **1**, **9** and **10**. (d–f) Photographs of the compounds **1**, **9** and **10** under natural light and UV lamp (365 nm) in solvents with varying polarity. (g–i) Emission spectra of compounds **1**, **9** and **10** in solvents with varying polarity (excited by the maximum absorption wavelength).

Table 3
Optical data for selected compounds in solvents with varying polarity.

Solvent	1			9			10		
	$\lambda_{abs,max}$ (nm) (ε/M^{-1} cm^{-1})	$\lambda_{em,max}$ (nm) [b] (Φ(%))	$\Delta\nu$ (cm^{-1})	$\lambda_{abs,max}$ (nm) (ε/M^{-1} cm^{-1})	$\lambda_{em,max}$ (nm) [b] (Φ(%))	$\Delta\nu$ (cm^{-1})	$\lambda_{abs,max}$ (nm) (ε/M^{-1} cm^{-1})	$\lambda_{em,max}$ (nm) [b] (Φ(%))	$\Delta\nu$ (cm^{-1})
CCl_4	450 (35,700)	543 (7.6)	3806	487 (27,300)	555 (75.2)	2516	/	/	/
Toluene	447 (34,800)	547 (4.1)	4090	492 (11,400)	568 (72.6)	2720	562 (11,000)	653 (41.1)	2480
o-Dichlorobenzen	456 (33,700)	552 (4.0)	3814	499 (42,600)	595 (58.3)	3233	591 (11,300)	695 (35.6)	2532
DCM	451 (29,600)	545 (1.2)	3824	494 (34,100)	606 (30.3)	3741	560 (30,500)	698 (30.4)	3530
Acetone	449 (28,500)	543 (1.4)	3856	491 (15,100)	611 (21.5)	4000	556 (6800)	707 (3.4)	3841
CH_3CN	449 (27,700)	543 (1.0)	3856	491 (11,300)	620 (12.1)	4238	525 (10,000)	722 (3.0)	5197
DMF	442 (31,200)	544 (1.6)	4242	501 (30,100)	628 (26.1)	4037	613 (17,400)	734 (4.1)	2689
DMSO	460 (35,500)	545 (0.7)	3391	506 (17,400)	644 (25.4)	4235	618 (9600)	749 (2.6)	2830

[a] Maximum absorption wavelength (10^{-5} mol/L).
[b] Maximum emission wavelength (excited by the maximum absorption wavelength) (10^{-5} mol/L).

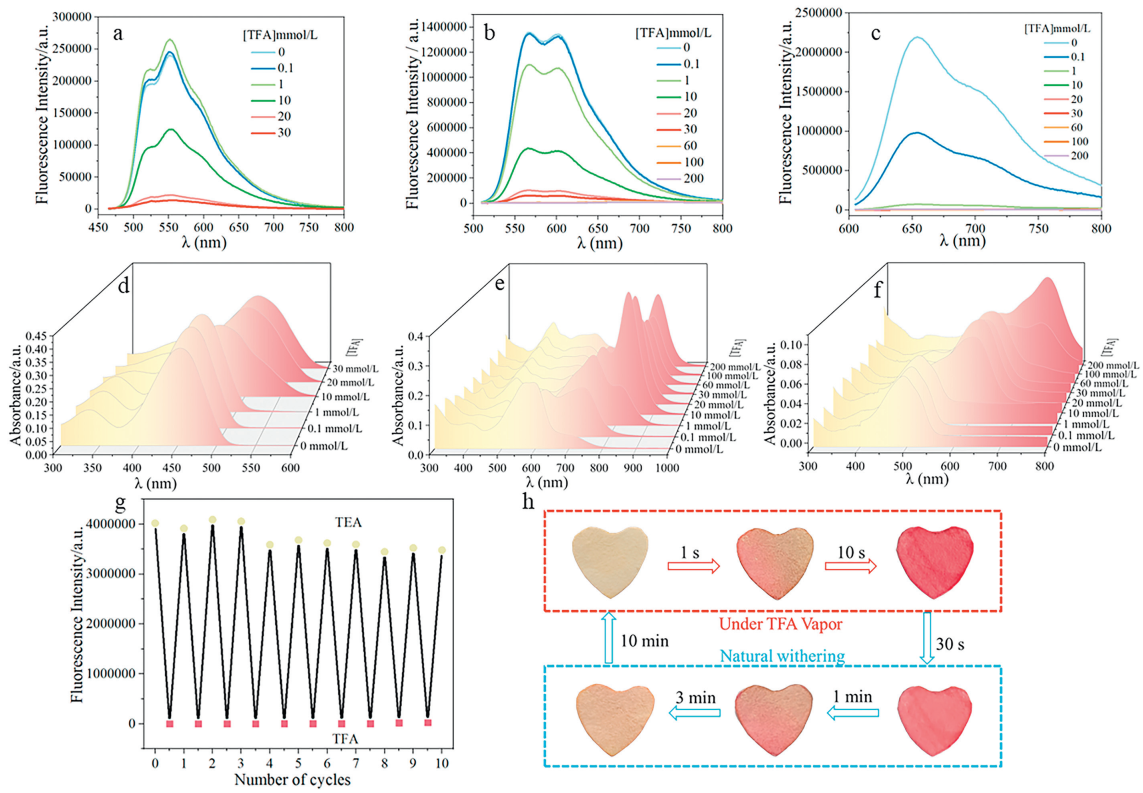

Fig. 6. (a–c) Emission spectra of compounds **1**, **9** and **10** in toluene with different trifluoroacetic acid concentration (excited by the maximum absorption wavelength). (d–f) Absorption spectra of compounds **1**, **9** and **10** in toluene with different trifluoroacetic acid concentration. (g) Reversible fluorescence intensity changes of compound **1** upon cycles of TFA-TEA treatments. (h) Photographs of compound **1** made into test paper for the detection of TFA vapor.

maximum emission wavelengths as the polarity of the solvent increased (Figs. 5e, f, h and i). The PLQY of compounds **1**, **9**, and **10** decreased as the solvent polarity increased. Compound **1** did not show a significant change in the Stokes shift with different polarities. However, compounds **9** and **10** displayed an increase in the Stokes shift as the solvent polarity increased. Notably, compound **10** had a maximum Stokes shift of 197 nm (Table 3). These large Stokes shifts and red-shifted fluorescence emissions hold great significance for biological applications [49]. This solvatochromic response can be attributed to the relaxes through interaction with the dipoles of solvent of the polar charge transfer excited states of compounds **9** and **10** in more polar solvents, resulting in larger Stokes shifts and redshifts. The new fluorophore's photostability is of great importance. It has been tested against fluorescein using compounds **1**, **9**, and **10**, and the results, as shown in Fig. S26 (Supporting information), indicate that it exhibits superior photostability (Figs. S42–S46 in Supporting information).

Trifluoroacetic acid (TFA) was chosen as the analyte to investigate the acid response behaviour of compounds **1**, **9**, and **10**. In toluene, the fluorescence intensity of compounds **1**, **9**, and **10** gradually decreased as the TFA concentration increased (Figs. 6a–c). Compound **1**, which appears as a yellow solution under nat-

ural light with a maximum absorption wavelength of 447 nm in toluene, exhibited a red-shifted absorption wavelength to 498 nm and changed from yellow to red with increasing TFA concentration (Fig. 6d and Fig. S47 in Supporting information). Similarly, when different concentrations of TFA were added, compounds **9** and **10** also showed a red-shifted maximum absorption wavelength of 712 nm and 835 nm, respectively (Figs. 6e and f, Figs. S49 and S51 in Supporting information). This change in absorption wavelength can be attributed to the nitrogen atom on the core biisoindolylidene and the alterations in H^+ binding, which affect the electron acceptance of the receptor. Consequently, a redshift in the maximum absorption wavelength occurs [50,51]. Interestingly, the luminescent behaviour of the compounds and the colour of the solution were restored when triethylamine was used as a base to neutralize TFA (Fig. 6g). This reversible colour change behaviour can be valuable for the detection of volatile acids (Fig. 6h). A test paper was prepared by immersing filter paper in a DCM solution containing compound **1** and then drying it. When exposed to TFA vapor, the colour of the paper changed significantly to red within 10 s. After allowing the TFA on the test paper to evaporate naturally, the paper returned to its original colour and could be reused.

In conclusion, a new class of fluorophores with a biisoindolylidene skeleton was successfully synthesized. The crystal structure analysis and DFT calculations revealed that these fluorophores have a rigid, conjugated, and coplanar structure and are excellent electron acceptors. To gain a deeper understanding of the photophysical properties of these fluorophores, a series of compounds with the biisoindolylidene backbone were synthesized, incorporating various electron-absorbing and electron-donating groups. This systematic approach allowed us to create a library of fluorescent probes with rational design. Furthermore, we investigated the solvatochromic effect and acid response of these compounds, and explored their potential application in detecting volatile acids. The development of these novel fluorophores holds promise for future biological research.

Declaration of competing interest

The authors declare that they have no known competing financial interests or personal relationships that could have appeared to influence the work reported in this paper.

CRediT authorship contribution statement

Xiaoyu Chen: Methodology, Investigation, Data curation. **Jiahao Hu:** Validation, Methodology. **Jingyi Lin:** Methodology. **Haiyang Huang:** Validation. **Changqing Ye:** Writing – review & editing, Writing – original draft, Visualization, Funding acquisition, Formal analysis, Data curation, Conceptualization. **Hongli Bao:** Writing – review & editing, Writing – original draft, Project administration, Funding acquisition, Data curation, Conceptualization.

Acknowledgment

This paper is dedicated to the memory of Dr G. W. A. Milne. This work was supported by the National Natural Science Foundation of China (Nos. 22225107, 22301302).

Supplementary materials

Supplementary material associated with this article can be found, in the online version, at doi:10.1016/j.cclet.2024.109923.

References

[1] S. Wang, W.X. Ren, J.T. Hou, et al., Chem. Soc. Rev. 50 (2021) 8887–8902.
[2] A.S. Klymchenko, Acc. Chem. Res. 50 (2017) 366–375.
[3] K. Pal, T. Dutta, A.L. Koner, ACS Omega 6 (2021) 28–37.
[4] J. Han, K. Burgess, Chem. Rev. 110 (2010) 2709–2728.
[5] A. Steinegger, O.S. Wolfbeis, S.M. Borisov, Chem. Rev. 120 (2020) 12357–12489.
[6] J. Yin, Y. Hu, J. Yoon, Chem. Soc. Rev. 44 (2015) 4619–4644.
[7] C. Li, H. Huang, L. Sun, et al., Angew. Chem. Int. Ed. 62 (2023) e202215436.
[8] M. Erard, S. Dupré-Crochet, O. Nüße, Am. J. Physiol. Regul. Integr. Comp. Physiol. 314 (2018) R667–R683.
[9] D. Wu, L. Chen, Q. Xu, X. Chen, J. Yoon, Acc. Chem. Res. 52 (2019) 2158–2168.
[10] S.C. Lee, J. Heo, H.C. Woo, et al., Chem. Eur. J. 24 (2018) 13706–13718.
[11] L.E. Santos-Figueroa, M.E. Moragues, E. Climent, et al., Chem. Soc. Rev. 42 (2013) 3489–3613.
[12] D. Wu, L. Chen, W. Lee, et al., Coord. Chem. Rev. 354 (2018) 74–97.
[13] H.W. Liu, L. Chen, C. Xu, et al., Chem. Soc. Rev. 47 (2018) 7140–7180.
[14] G.S. Loving, M. Sainlos, B. Imperiali, Trends Biotechnol. 28 (2010) 73–83.
[15] X. Guo, N. Yang, W. Ji, et al., Adv. Mater. 33 (2021) e2007778.
[16] H. Zhu, J. Fan, J. Du, X. Peng, Acc. Chem. Res. 49 (2016) 2115–2126.
[17] K.N. Wang, L.Y. Liu, D. Mao, et al., Angew. Chem. Int. Ed. 60 (2021) 15095–15100.
[18] N. Amdursky, Y. Erez, D. Huppert, Acc. Chem. Res. 45 (2012) 1548–1557.
[19] Z.R. Grabowski, K. Rotkiewicz, W. Rettig, Chem. Rev. 103 (2003) 3899–4032.
[20] A.C. Sedgwick, L. Wu, H.H. Han, et al., Chem. Soc. Rev. 47 (2018) 8842–8880.
[21] G. Lukinavičius, L. Reymond, K. Umezawa, et al., J. Am. Chem. Soc. 138 (2016) 9365–9368.
[22] G. Lukinavičius, K. Umezawa, N. Olivier, et al., Nat. Chem. 5 (2013) 132–139.
[23] F. Wurthner, T.E. Kaiser, C.R. Saha-Moller, Angew. Chem. Int. Ed. 50 (2011) 3376–3410.
[24] R.T.K. Kwok, C.W.T. Leung, J.W.Y. Lam, B.Z. Tang, Chem. Soc. Rev. 44 (2015) 4228–4238.
[25] J. Mei, N.L.C. Leung, R.T.K. Kwok, J.W.Y. Lam, B.Z. Tang, Chem. Rev. 115 (2015) 11718–11940.
[26] S. Tong, J. Dai, J. Sun, et al., Nat. Commun. 13 (2022) 5234.
[27] Y. Goto, S. Omagari, R. Sato, et al., J. Am. Chem. Soc. 143 (2021) 14306–14313.
[28] F. Gu, Y. Li, T. Jiang, J. Su, X. Ma, CCS Chem. 4 (2022) 3014–3022.
[29] X. Luo, J. Li, J. Zhao, et al., Chin. Chem. Lett. 30 (2019) 839–846.
[30] C. Reichardt, Chem. Rev. 94 (2002) 2319–2358.
[31] Y. Niko, A.S. Klymchenko, J. Biochem. 170 (2021) 163–174.
[32] E. Benedetti, L.S. Kocsis, K.M. Brummond, J. Am. Chem. Soc. 134 (2012) 12418–12421.
[33] B.E. Cohen, T.B. McAnaney, E.S. Park, et al., Science 296 (2002) 1700–1703.
[34] G.G. Talanova, V.S. Talanov, Supramol. Chem. 22 (2010) 838–852.
[35] Z. Lu, S.J. Lord, H. Wang, W.E. Moerner, R.J. Twieg, J. Org. Chem. 71 (2006) 9651–9657.
[36] O.A. Kucherak, P. Didier, Y. Mély, A.S. Klymchenko, J. Phys. Chem. Lett. 1 (2010) 616–620.
[37] Y. Niko, P. Didier, Y. Mely, G. Konishi, A.S. Klymchenko, Sci. Rep. 6 (2016) 18870.
[38] Y. Niko, S. Kawauchi, G.i. Konishi, Chem. Eur. J. 19 (2013) 9760–9765.
[39] P. Venkatraman, T.T. Nguyen, M. Sainlos, et al., Nat. Chem. Biol. 3 (2007) 222–228.
[40] P.B. Ghosh, J. Chem. Soc. B 0 (1968) 334–338.
[41] Z. Diwu, Y. Lu, C. Zhang, D.H. Klaubert, R.P. Haugland, Photochem. Photobiol. 66 (2008) 424–431.
[42] Z. Lu, N. Liu, S.J. Lord, et al., Chem. Mater. 21 (2009) 797.
[43] O.A. Kucherak, L. Richert, Y. Mely, A.S. Klymchenko, Phys. Chem. Chem. Phys. 14 (2012) 2292–2300.
[44] W. Huang, S. Feng, J. Liu, et al., Angew. Chem. Int. Ed. 62 (2023) e202219337.
[45] C. Ye, R. Huang, M.F. Chiou, et al., Chem. Sci. 14 (2023) 13151–13158.
[46] S. Xu, H. Huang, C. Yuan, et al., Org. Chem. Front. 8 (2021) 1747–1755.
[47] P.J. Stephens, F.J. Devlin, C.F. Chabalowski, M.J. Frisch, J. Phys. Chem. A 98 (1994) 11623–11627.
[48] C.H. Lim, M.D. Ryan, B.G. McCarthy, et al., J. Am. Chem. Soc. 139 (2017) 348–355.
[49] M.V. Sednev, V.N. Belov, S.W. Hell, Methods Appl. Fluoresc. 3 (2015) 042004.
[50] C. Jin, K. Li, J. Zhang, Z. Wang, J. Tan, Chin. Chem. Lett. (2024) 109532.
[51] J. Liu, W. Huang, B. Liang, et al., Chem. Mater. 34 (2022) 9492–9502.